

Conference Paper

Influence of Heat Treatment After Arc Discharge Route on Structure and Loading Capacity of SBA-15 Encapsulated By Iron Particles

M Ulfa¹, T E Saraswati², and B Mulyani¹¹Chemical Education Study Program, Faculty of Teacher Training and Education, Universitas Sebelas Maret, Jl. Ir. Sutami 36A, Surakarta 57126, Central Java Indonesia²Department of Chemistry, Faculty of Mathematics and Natural Sciences, Universitas Sebelas Maret, Jl. Ir. Sutami 36A, Surakarta 57126, Central Java Indonesia

Abstract

For the first time, the influence of heat treatment on the structure of SBA-15 encapsulated iron particle has been investigated after arc discharge methods. Molecular sieve silica SBA-15 was prepared by self-assembly route using block copolymer P123 as soft templating agent and tetraethoxysilane as silica precursor involving acid treatment. Arc discharge route was followed by heat-treatment of SBA-15 for 4 h at 400, 700 and 900 °C. The change of sample structure was studied by X-ray diffraction, scanning electron microscopy and nitrogen adsorption-desorption techniques, VSM and FTIR. It is found that after arc discharge step, the magnetic properties of SBA-15 encapsulated iron particle reached stable crystal at high temperature. In the other way, the massive structural change in a significant part of SBA-15 encapsulated iron particle during high temperature had an impact on the decreased surface area, total pore volume, and post size distribution. The loading capacity performance of SBA-15 encapsulated iron particle was investigated by ibuprofen molecule impregnation as a drug model. The result showed that high-temperature treatment of SBA-15 encapsulated iron particle decreased the loading capacity which was firmly related to the shrinkage of mesoporous nanopipe of SBA-15.

Corresponding Author:

M Ulfa

ulfa.maria2015@gmail.com

Received: 23 February 2019

Accepted: 6 March 2019

Published: 25 March 2019

Publishing services provided by
Knowledge E

© M Ulfa et al. This article is distributed under the terms of the [Creative Commons Attribution License](#), which

permits unrestricted use and redistribution provided that the original author and source are credited.

Selection and Peer-review under the responsibility of the ICO-HELICS Conference Committee.

1. Introduction

Mesoporous silica SBA-15 is one of the attractive materials that can be used for many applications, such as adsorption, separation, catalysis, and energy storage devices [1]. The unique properties of mesoporous silica SBA-15 such as honeycomb structure, high thermal and chemical stability, large surface area, and high pore volume influenced their popularity [2]. The endotemplating method is the most popular route that has been used for the synthesis of mesoporous silica SBA-15 in which the silica precursor is filled

OPEN ACCESS

with a soft template that decomposes during heating treatment for silica wall formation [3]. The problematic route and high energy consumption impacted to the high cost of mesoporous silica SBA-15. For this reason, regeneration of mesoporous silica SBA-15 is an important point for economic and energy saving.

Mesoporous silica SBA-15 modification has a significant influence on the regeneration point of view. Magnetization is one of flexible technique that can be employed to regenerate improvement for mesoporous silica SBA-15 [4-5]. Many different metals such as iron, cobalt, nickel, including on ionic form and solid state form had been applied as metal precursors that encapsulated into mesoporous silica SBA-15 surface in the previous reports [6-8]. Many techniques such as impregnation, sonication, and microwave have been employed as encapsulation methods [9-10]. However, these methods are not successful yet to form a high magnetic character on mesoporous silica SBA-15.

In the present study, a mesoporous silica SBA-15 modified by iron has been employed. Mesoporous silica SBA-15 was synthesized by pluronic P123 as a template. The iron encapsulation on mesoporous silica SBA-15 was obtained using the arc-discharge method. For studying the influences of temperature, all the sample were heated by varying temperature. After the iron encapsulation on mesoporous silica SBA-15 synthesis, the character of their structure was investigated by X-ray diffraction, scanning electron microscopy and nitrogen adsorption-desorption techniques, VSM and FTIR. The loading capacity of the sample was studied by adsorption using ibuprofen as adsorbate model.

2. Material and Method

2.1. Material

All reagents and solvents were of analytical grade, including a co-block polymer (P123), tetraethylorthosilicate (TEOS), ethanol, hydrochloric acid, and deionized water purchased from Aldrich. Ibuprofen, n-, and FeCl_3 were purchased from Sigma.

2.2. Synthesis of silicas mesoporous silica SBA-15

Mesoporous silica SBA-15 was prepared in the presence of non-ionic co-block polymer (P123) surfactant. This was synthesized according to the route described by Zhao *et al.* [11] with a modification during the hydrothermal process. Pluronic P123 was dissolved in distillation water at room temperature, followed by adding 2M hydrochloric acid solution, then it was kept on stirring condition for 24 h. The mass ratio of P123: TEOS: HCl is

0.4:15.0:1.0 (%w/v/v). TEOS was dropped into the first resulting solution in stirring at room temperature for 24 h. The resulting mixture was carried out into a hydrothermal reactor at 100 °C for 24 h, followed by filtering, washing and drying at 100 °C for 24 h. At the end of the experiment, the white powder was calcinated at 600 °C for 4 h.

2.3. Synthesis of SBA-15 encapsulated by iron particles

Encapsulation of mesoporous silica SBA-15 with iron is prepared according to the route described by Chaitoglou *et al* [11] with a modification during the heating process. Iron/SBA-15 was obtained first from the iron oxide electrolysis process (40 to 70 A for 2 h) using 0.375 M NaCl as an electrolyte. Chlorine ion had been removed by AgNO₃ solution on the filtrate, followed by a heating process at a temperature of 250 °C for 1 h to obtain filler. The magnetic material was made from carbon (graphite), silica glue (as a binder), SBA-15 and ethanol with a mass ratio of 1:3:1:0.01 (w/w). A solid graphite tube measuring 50 mm in length with a diameter of 10 mm was used as a cathode. Anode and cathode were cultivated closely in a minimal distance but not sticking to each other. This was done in order to facilitate the electric jump that was marked by sparks. The current and the electrodes (both the anode and the cathode) were set up in the beaker glass containing the urea p.a solution (Merck) in ethanol. The current used in this method is 10 A. This process took place from the first appearance of sparks until there were no longer visible sparks in the time between 10-15 min. The solution medium was used in 50% ethanol arc-discharge. The final product was labeled as Fe/SBA-15. Each sample was heated at 400 °C, 700 °C and 900 °C for 4 h, then labeled as Fe/SBA-15-400, Fe/SBA-15-700, and Fe/SBA-15-900.

2.4. Ibuprofen loading

The ibuprofen-loaded Fe/SBA-15 materials were prepared by impregnation method. Fe/SBA-15 material was suspended in 50 ppm ibuprofen on n-hexane. The mixture was kept at freezer for 2 days in a closed batch. The resulting solids were washed with hexane, filtered with Whatman paper 41 and dried at 60 °C for 24 h. The ibuprofen-loaded Fe/SBA-15 were analyzed by XRD, nitrogen adsorption-desorption, FTIR, and SEM.

2.5. Characterization

The Fe/SBA-15 materials were characterized through Fourier transform infrared spectroscopy by Shimadzu FTIR instrument. The microscopic features of the samples were observed with a field-emission scanning electron microscope (SEM) (JSM-6700F, JEOL Japan) operated at 10 kV. The XRD patterns of the Fe/SBA-15 were recorded with a Bruker D8-Advance powder diffractometer using Ni-filtered Cu-K α radiation ($k = 1.54056 \text{ \AA}$) over a two theta range of 10–80°. Nitrogen adsorption-desorption isotherms were performed at 196 °C using a Nova instrument.

3. Results and Discussion

Figure 1 shows the scanning electron microscopy (SEM) image of Fe/SBA-15-400 and Fe/SBA-15-900 samples. As can be seen in Figure 1, all of the samples were clearly described a pipe-like structure with a diameter range of the iron oxide particles of 0.1–0.4 μm and the length in the range of 10–20 μm . The iron oxide was distributed with high homogeneity without any significant overlapping coated layered by iron. The Fe/SBA-15-900 sample is sharper than Fe/SBA-15-400. This fact indicates that high heat treatment serves a significant impact for the crystallization process. The Fe/SBA-15-400 samples have a larger amorphous part than Fe/SBA-15-900 due to the crystal formation in high temperature. The differences in the surface of Fe/SBA-15 sample were described genuinely by FTIR.

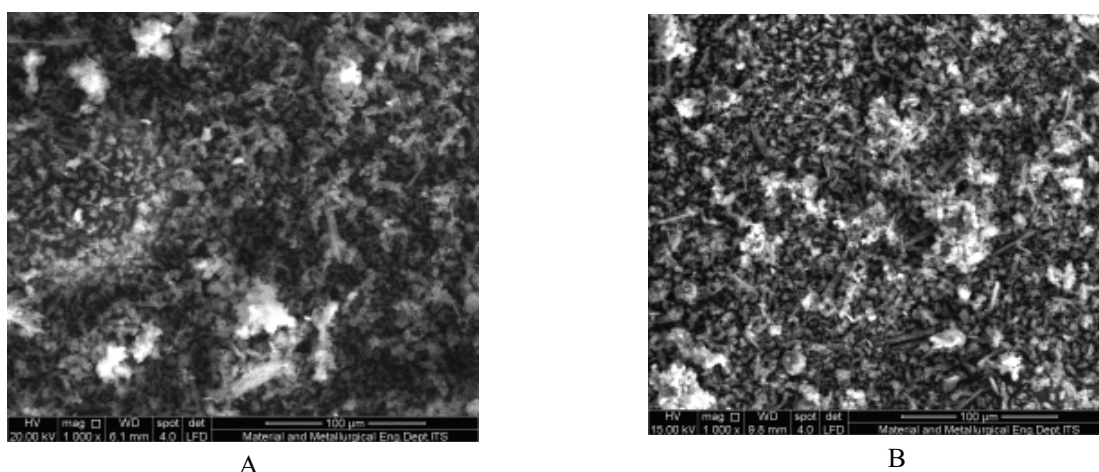


Figure 1: Scanning electron microscope image of Fe/SBA-15 by arc-discharge after heating treatment at (A) 400 °C and (B) 900 °C for 4 h.

Figure 2 shows the functional group of all samples analyzed by FTIR. The functional groups containing oxygen are observed at 3600-3200 cm^{-1} that were assigned as

stretching vibrations of the O-H bonds of silanol. A large number of water adsorbed on Fe/SBA-15 sample was observed by broadening peak at $3600\text{-}3400\text{ cm}^{-1}$. The stretching vibration of the Si-O-Si was clearly observed at $1200\text{-}100\text{ cm}^{-1}$. The band within the range of $850\text{-}800\text{ cm}^{-1}$ was derived from the stretching vibrations of the Fe-O bonds present in the iron oxide form. As can be seen, the silanol peak at $3600\text{-}3200\text{ cm}^{-1}$ of Fe/SBA-15-900 was the smallest of all samples which indicated the decreasing amount of water adsorbed on the sample surface due to the high-temperature treatment after iron encapsulation. The peak of Si-O-Si was still observed in all samples which indicated that mesoporous silica SBA-15 was still stable after high-temperature treatment. On the other side, the peak of Fe-O was decreased with increasing temperature which indicated that the iron precursor replaced the iron particle at high temperature. This prediction was evident in XRD pattern.

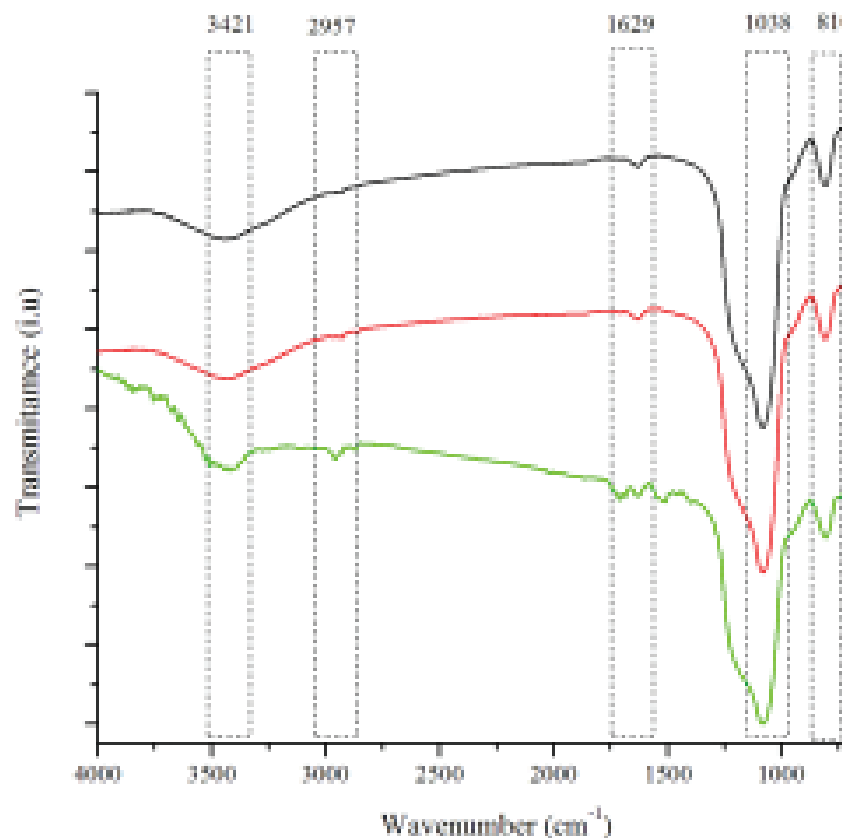


Figure 2: FTIR of Fe/SBA-15 by arc-discharge after heating treatment at $400\text{ }^{\circ}\text{C}$ (black), $700\text{ }^{\circ}\text{C}$ (red) and $900\text{ }^{\circ}\text{C}$ (green) for 4 h.

Figure 3 shows XRD profiles of the Fe/SBA-15 samples. As can be seen at Figure 3, the hexagonal $p2mm$ symmetry observed at 200 reflections in 2θ 26.5° . The iron peaks observed at 2θ were 35.9186° , 57.5602° and 63.2059° which had good agreement with JCPDS No. 89-0597 and JCPDS No. 39-1346 for Fe_2O_3 hematite, Fe_3O_4 magnetite,

and $\gamma\text{-Fe}_2\text{O}_3$, respectively. The clear reflection of 26.5° in sample Fe/SBA-15-400 and Fe/SBA-15-900 indicated that mesoporous silica framework had good physical stability even when they were treated at high treatment. For iron case, the high treatment of Fe/SBA-15-900 sample had the most significant impact for decreasing magnetite peaks at 35.9186° and 57.5602° . In our prediction, the iron particle was agglomerated more massively at a higher temperature than a lower temperature due to increasing packing degree as temperature driving force. The new phenomenon was also confirmed by the differences in the peak intensities of iron and silica peak on XRD. This difference indicated that iron incorporation did not destruct the ordering of mesoporous silica SBA-15 materials due to the high thermal stability of SBA-15. Pore properties of Fe/SBA-15 described the other evidence in nitrogen adsorption-desorption result.

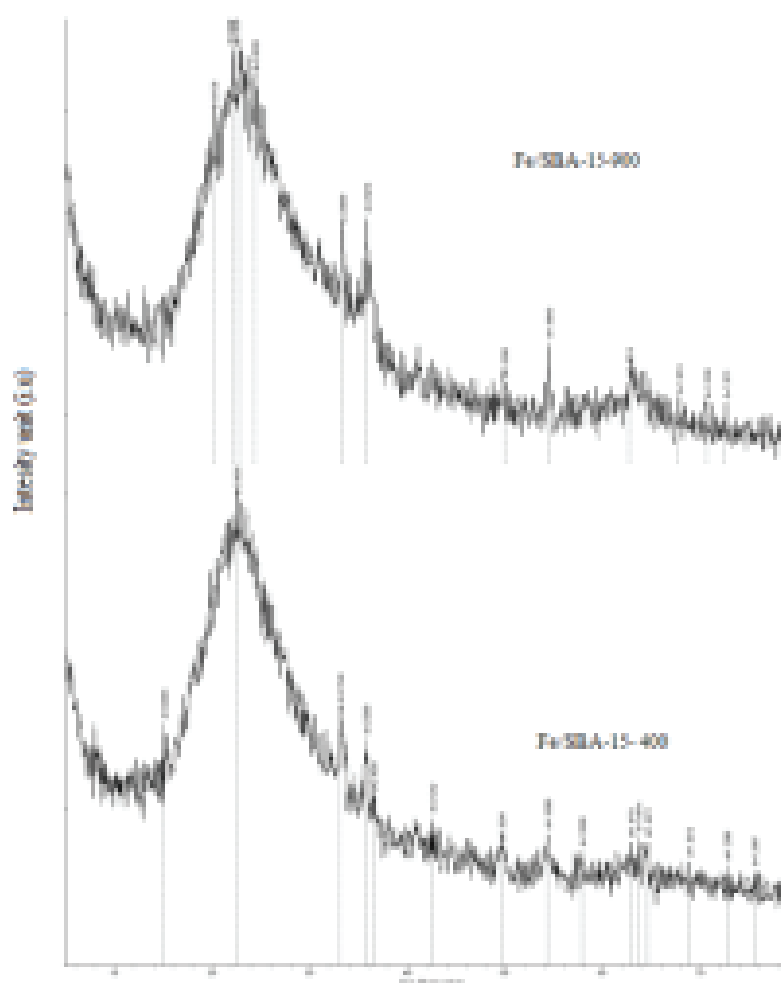


Figure 3: XRD result of Fe/SBA-15 by arc-discharge after heating treatment at 400°C (below) and 900°C (above) for 4 h.

Figure 4 shows the nitrogen adsorption-desorption isotherm for SBA-15 and Fe/SBA-15-900. The pore type of all samples was clearly described by isotherms type IV with

almost vertical hysteresis loop which is attributed as mesoporous type. The ordering pores of all samples were indicated by the sharp inflection in relative pressure range of 0.4-0.7 as capillary condensation. The differences of hysteresis loop were found on decreased sharp inflection on Fe/SBA-15 sample which is indicated the decreasing of not only the pore uniformity but also the surface area. In our expectation, this phenomenon occurred because a large number of mesopore part of SBA-15 had been covered by iron particle during the encapsulation process. The second reason is that the mesoporous silica SBA-15 framework was condensed by high-temperature treatment which had a great impact on the silica and iron shrinkage. The surface area of SBA-15 ($550 \text{ m}^2/\text{g}$) is higher than Fe/SBA-15 ($370 \text{ m}^2/\text{g}$) due to the iron covering and heat driving force. However, the Fe/SBA-15 sample still maintain not only the SBA-15 framework but also its iron character in high temperature. On ibuprofen adsorption experiment, the loading capacity of Fe/SBA-15-400 (130 mg/g) is higher than Fe/SBA-15-900 (105 mg/g). In our assumption, the decreasing surface areas was the result of the high-temperature that decreased the loading capacity. As a previous explanation in SEM, FTIR and XRD result, the textural properties of Fe/SBA-15-900 were decreased but the crystal part was increased along with the increasing temperature treatment. The best news of Fe/SBA-15-900 is that it maintained its ordering structure with the magnetic character which is described by VSM.

Figure 4 shows the hysteresis curve of Fe/SBA-15-900 by VSM. The applied magnetic field was demonstrated by hysteresis curves that described the magnetic moment of Fe/SBA-15-900. The intersection of the magnetization curve and $y=0$ axis represented the remanent coercivity. The coercivity of the bulk cylinder sample is 16.5 mT. The differences in spin magnetization were irregular due to the interaction between iron ion and oxygen in silica surface as the magnetization of Fe/SBA-15 was lower than iron oxide as a precursor. The exciting information from Figure 2 is the superparamagnetic properties of Fe/SBA-15 with a magnetization value of 7.9 emu/g .

4. Conclusion

Encapsulation of mesoporous silica SBA-15 with iron particle has been successfully prepared by arc-discharge method followed by heat treatment for 4 h at 400, 700 and 900 °C. The change of sample structure was observed by X-ray diffraction, scanning electron microscopy and nitrogen adsorption-desorption techniques, VSM and FTIR. The magnetic properties and textural framework of Fe/SBA-15-900 were higher than Fe/SBA-15-400 due to the increasing crystallinity of material at high temperature. The loading

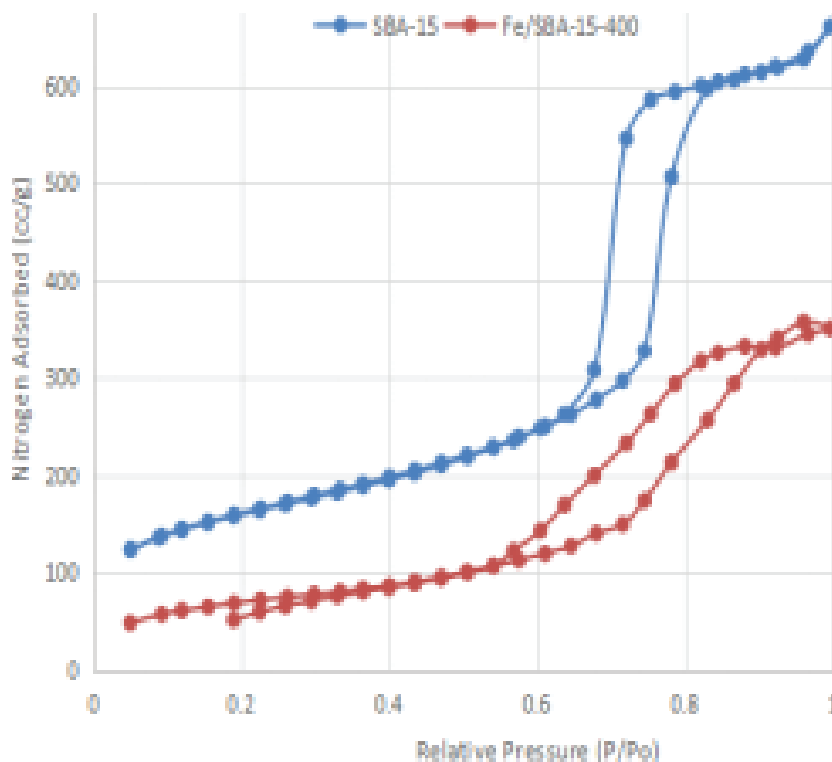


Figure 4: The isotherm result of SBA-15 and Fe/SBA-15-900 after ibuprofen loading process.

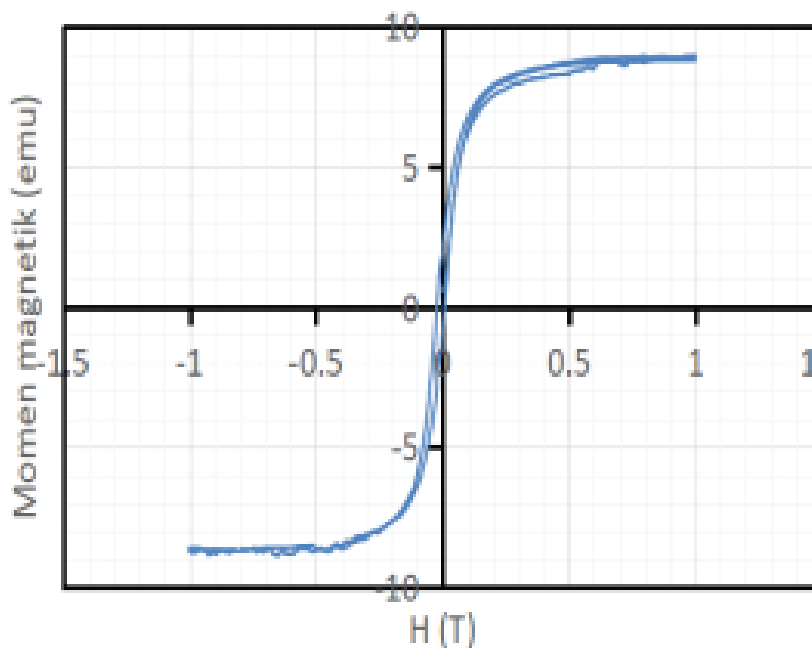


Figure 5: Magnetization result of Fe/SBA-15 by arc-discharge after heating treatment at 900 °C for 4 h; analyzed by VSM.

capacity of Fe/SBA-15-900 is lower than Fe/SBA-15-400 as the impact on decreasing surface area, total pore volume, and pore size distribution due to the shrinkage of mesoporous nanopipe of SBA-15. As the summary, Fe/SBA-15-900 is the best material for

ibuprofen separation process due to the magnetic effect but not favorable for adsorption field.

Acknowledgment

We gratefully acknowledge the financial support from the PNBP UNS under Fundamental Research Grant 2018 with contract number of grant 543/UN27.21/PP/2018.

References

- [1] Nejad F N, Shams E, Amini M K, and Bennett J C 2013 *Microporous Mesoporous Mater.* **2** 239-46
- [2] Ulfa M, and Jannah A M 2018 *Oriental J. Chem.* **341** 420–29
- [3] Luan Z and Fournier, J A, 2005 *Microporous Mesoporous Mater.* **79** 1–3, 235–40
- [4] Havránek A and Zemánek, I, 2017 *J. Magn. Magn.Mater.* **443** 137–41
- [5] Yu A, Niu W, Hong X, He Y, Wu M, Chen Q, and Ding M 2018 *Tribol. Int.* **57** 84–93
- [6] Kletetschka G 2018 *Earth Planet. Sci. Lett.* **487** 1–8
- [7] Du J, Liu X, Qin H, Wei Z, Kong X, and Liu Q 2018 *Physica C: Supercond.* **547** 1–6
- [8] Khedr DM, Aly S H, Shabara R M, and Yehia S 2017, *J.Magn. Magn.Mater.* **430** 103–8
- [9] Kumari R, Singh A, Yadav BS, Ranjan, D, Ghosh, A, Guha, P, Tyagi, P K 2017 *Carbon* **119** 464–75
- [10] Eremina R, Seidov Z, Ibrahimov I, Najafzade M, Aljanov M and Mamedov, D 2017 *J. Magn. Magn. Mater.* **440** 179–80
- [11] DY Zhao J L, Feng QS, Huo N, Melssoh G H, Fredrickson BF, Chmelka GD 1998 *Science* **279** 548–52
- [12] Chaitoglou S, Sanaee M R, Aguayo N, Bertran E 2014 *J. Nanomater.* **32** 34